Epitaxial growth of the first five members of the $Sr_{n+1}Ti_nO_{3n+1}$ Ruddlesden–Popper homologous series

J. H. Haeni, C. D. Theis, and D. G. Schlom[a]
Department of Materials Science and Engineering, The Pennsylvania State University, University Park, Pennsylvania 16802-5005

W. Tian and X. Q. Pan
Department of Materials Science and Engineering, The University of Michigan, Ann Arbor, Michigan 48109-2136

H. Chang, I. Takeuchi,[b] and X.-D. Xiang
Materials Sciences Division, Lawrence Berkeley National Laboratory, Berkeley, California 94720

The first five members of the $Sr_{n+1}Ti_nO_{3n+1}$ Ruddlesden–Popper homologous series, i.e., Sr_2TiO_4, $Sr_3Ti_2O_7$, $Sr_4Ti_3O_{10}$, $Sr_5Ti_4O_{13}$, and $Sr_6Ti_5O_{16}$, have been grown by reactive molecular beam epitaxy. A combination of atomic absorption spectroscopy and reflection high-energy electron diffraction intensity oscillations were used for the strict composition control necessary for the synthesis of these phases. X-ray diffraction and high-resolution transmission electron microscope images confirm that these films are epitaxially oriented and nearly free of intergrowths. Dielectric measurements indicate that the dielectric constant tensor coefficient ϵ_{33} increases from a minimum of 44 ± 4 in the $n=1(Sr_2TiO_4)$ film to a maximum of 263 ± 2 in the $n=\infty(SrTiO_3)$ film. © *2001 American Institute of Physics.* [DOI: 10.1063/1.1371788]

The controlled synthesis of a wide variety of homologous oxide crystal systems offers tremendous potential for tailoring the superconducting, ferroelectric, and dielectric properties of materials. Although much progress has been made in growing some superconducting homologous series phases by molecular beam epitaxy (MBE),[1–3] intergrowths continue to prohibit the phase-pure growth of many of these systems.[4,5] These intergrowths inhibit the identification of the electrical properties of individual members of these series. Similarly, intergrowths are seen in many dielectric homologous series[6] and prevent the investigation of dielectric constant, dielectric loss, and dielectric tunability in the higher order members.

The $n=\infty$ member of the $Sr_{n+1}Ti_nO_{3n+1}$ Ruddlesden–Popper homologous series,[7] $SrTiO_3$, exhibits a wide range of electrical behavior: from a high dielectric constant tunable paraelectric in its undoped form, to a metallic superconductor when doped with a variety of elements. It has been studied as a substrate for perovskite oxides and for application in tunable dielectric devices,[8,9] dynamic random access memory, and as an alternative gate oxide in metal–oxide–semiconductor field effect transistors (MOSFETs).[10]

This broad range of physical properties and applications of $SrTiO_3$ make the investigation of the properties of other members of this homologous series (Fig. 1) an obvious step in the search for new materials with improved properties. For example, polycrystalline samples of Sr_2TiO_4 ($n=1$) and $Sr_3Ti_2O_7$ ($n=2$) exhibit lower dielectric loss than $SrTiO_3$.[11–12] Unfortunately, the study of these phases has been limited by several factors. First, $SrTiO_3$ is the only

member of the series that melts congruently.[13] The single crystal growth of Sr_2TiO_4 is complicated (if not prohibited) by a phase transition at 1550 °C and a peritectic decomposition at 1860 °C.[13] $Sr_3Ti_2O_7$ has a peritectoid decomposition at 1580 °C,[13] which prohibits growth of single crystals of this phase from the melt.

Conventional solid state techniques have been successful in making (polycrystalline) samples of only the $n=1-3$ members.[7,14] Previous attempts to synthesize intermediate ($3<n<\infty$) members of this series have been unsuccessful.[6] This has been explained by lattice energy calculations performed by several groups.[15–17] The results of the calculations from all groups are in agreement that there is no driving force to form single-phase samples with intermediate n.[15–17] Due to the slight differences in calculated energies, however, there is some disagreement as to which phases are stable and
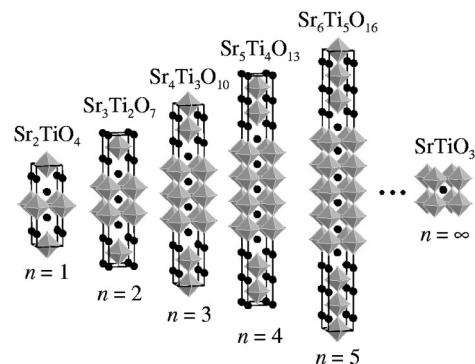

FIG. 1. Schematic of the crystal structure of a unit cell of the $n=1$ (Sr_2TiO_4), $n=2$ ($Sr_3Ti_2O_7$), $n=3$ ($Sr_4Ti_3O_{10}$), $n=4$ ($Sr_5Ti_4O_{13}$), $n=5$ ($Sr_6Ti_5O_{16}$), and $n=\infty$ ($SrTiO_3$) members of the $Sr_{n+1}Ti_nO_{3n+1}$ Ruddlesden–Popper homologous series. Circles represent Sr atoms, while Ti atoms are at the center of the octahedra (coordination polyhedra) with oxygen atoms at each apex.

[a]Electronic mail: schlom@ems.psu.edu
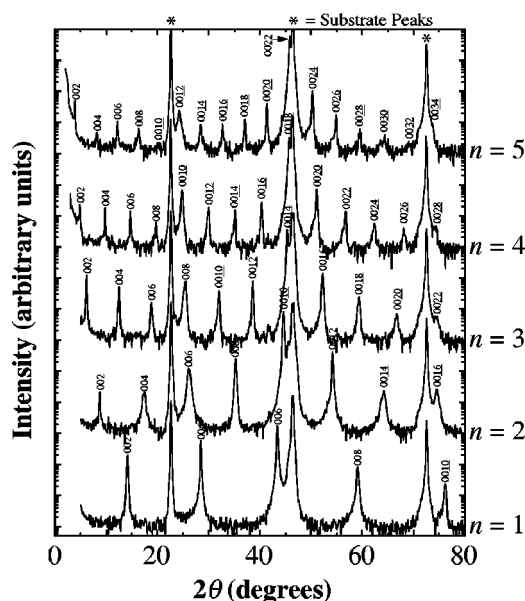[b]Present address: Department of Materials and Nuclear Engineering, University of Maryland, College Park, MD 20742.

FIG. 2. θ–2θ x-ray diffraction scans of the first five members of the $Sr_{n+1}Ti_nO_{3n+1}$ Ruddlesden–Popper homologous series grown on SrTiO$_3$ (001) substrates. Substrate peaks are labeled with a (*), and the plots are offset for clarity. The narrow peaks at the correct 2θ positions indicate that each of the films is single phase.

which are metastable. For example, McCoy *et al.*[16] concluded that $Sr_3Ti_2O_7$ and SrTiO$_3$ are the only stable $Sr_{n+1}Ti_nO_{3n+1}$ phases, whereas Noguera[17] concluded that Sr_2TiO_4, $Sr_3Ti_2O_7$, and SrTiO$_3$ are the only stable phases.

We have used MBE to overcome these challenging barriers to the synthesis of these materials. Each of the unit cells of this series is made up of different sequences of SrO and TiO$_2$ layers (Fig. 1). SrTiO$_3$ has the perovskite crystal structure with alternating TiO$_2$ and SrO layers; we refer to the combination of these two layers as a perovskite sheet. The $n=1$ (Sr_2TiO_4) compound has an additional SrO layer (making a double SrO layer) disrupting each perovskite sheet along the c axis. Subsequent members of the series have an increasing number of perovskite sheets separated by the double SrO layers. By changing the shuttering sequence of Sr and Ti ions to match the layering sequence of the desired phase, we have grown epitaxial films of these phases despite the fact that they melt incongruently, have structural transitions, and lack sufficient driving forces for formation.

The $n=1$–5 members of this series were grown using an oxide MBE system. Before growth, the substrates were etched with a buffered HF solution to achieve a TiO$_2$-terminated surface.[18] Monolayer doses (6.6×10^{14} atoms/cm^2) of Sr and Ti were deposited in a sequential manner on well oriented ($\pm 0.1°$) SrTiO$_3$(001) substrates. For the double-SrO layers in these structures, a dose corresponding to twice the monolayer dose was delivered. The average flux of both the Sr and Ti sources was 1.0×10^{14} atoms/cm$^2 \cdot$s for all growths. During growth, the substrate temperature was 750 °C as measured by an optical pyrometer. The substrate was immersed in a continuous flux of molecular oxygen, yielding a background pressure of 2×10^{-7} Torr. The thicknesses of the films were 470, 410, 565, 540, and 590 Å, for the $n=1$–5 films, respectively.

A combination of reflection high-energy electron diffraction (RHEED) intensity oscillations and atomic absorption spectroscopy (AA) was used to adjust the stoichiometry of the Sr and Ti molecular beams and ensure that a complete monolayer of each cation was deposited in each shuttered cycle.[19] A series of growths revealed that the phase-pure synthesis of these compounds required that both the stoichiometry and absolute monolayer doses not be off by more than about 1%.

Films grown outside this narrow composition window (i.e., where the stoichiometry or absolute monolayer doses are off by more than 1%) show clear evidence of intergrowths within the desired phase when examined by x-ray diffraction. A nonperiodic stacking sequence in the c direction (intergrowths) causes certain x-ray peaks to split, broaden, or shift in 2θ.[20,21] The monolayer-by-monolayer deposition of films with the correct stoichiometry resulted in single-phase films whose x-ray peaks show narrow widths and the correct 2θ positions (Fig. 2). The c-axis lattice constant of these phases as determined by a Nelson–Riley[22] analysis of the diffraction peak positions is 12.46 ± 0.02 Å, 20.35 ± 0.05 Å, 28.1 ± 0.2 Å, 35.6 ± 0.2 Å, and 43.5 ± 1.0 Å for the $n=1$–5 phases, respectively. This compares to the bulk reported lattice constants of 12.601, 20.38, and 28.1 Å for the $n=1$–3 phases, respectively.[7] X-ray ϕ scans of the 103, 105, 107, 109 and 10$\underline{11}$ peaks of the $n=1$–5 films, respectively, indicated epitaxial, c-axis films with orientation (001)$Sr_{n+1}Ti_nO_{3n+1}\|$(001)SrTiO$_3$ and [100]$Sr_{n+1}Ti_nO_{3n+1}\|$[100]SrTiO$_3$.[23] The in-plane lat-

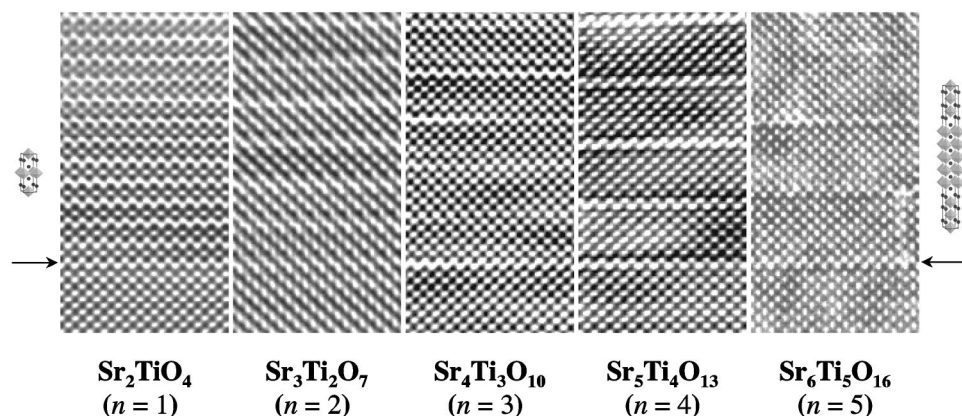| Sr_2TiO_4	$Sr_3Ti_2O_7$	$Sr_4Ti_3O_{10}$	$Sr_5Ti_4O_{13}$	$Sr_6Ti_5O_{16}$
($n=1$)	($n=2$)	($n=3$)	($n=4$)	($n=5$)

FIG. 3. Cross-sectional HRTEM images (from left to right) of the $n=1$ (Sr_2TiO_4), $n=2$ ($Sr_3Ti_2O_7$), $n=3$ ($Sr_4Ti_3O_{10}$), $n=4$ ($Sr_5Ti_4O_{13}$), and $n=5$ ($Sr_6Ti_5O_{16}$) films. A model of the crystal structure of the $n=1$ and $n=5$ members are adjacent to the corresponding images showing the position of the SrO double layers and perovskite layers. The arrows mark the position of the interface of the films with the homoepitaxial SrTiO$_3$ buffer layer.

tice constants determined from the x-ray measurements ranged from 3.83 ± 0.05 Å to 3.94 ± 0.05 Å.[23]

A JEOL 4000EX high-resolution transmission electron microscope (HRTEM) operated at 400 kV was used to examine the local nanostructure of these films.[23] Figure 3 is a cross-sectional HRTEM image showing the interface of each of these phases with the $SrTiO_3$ homoepitaxial buffer layer. Equal spacing between the double SrO layers (light lines) indicates a single-phase film. All of the imaged areas of the $n = 1-3$ films look similar to the region shown in Fig. 3 with no intergrown regions observed. However, some intergrowths of higher n phases were observed in localized regions of the $n = 4$ and 5 films. In addition, defects consisting of vertical SrO double layers (see Fig. 3) were commonly seen adjacent to an intergrowth.[23] Such vertically running SrO double layers have also been seen in bulk $Sr_{n+1}Ti_nO_{3n+1}$ samples and have been shown to have low-energy interfaces.[16] They have also been observed in other perovskite homologous series.[20,24–26] The intergrowths in these samples are most likely the result of slight monolayer-to-monolayer composition fluctuations during the deposition of the films. These ($<1\%$) fluctuations are present in all of the growths, but the higher n phases seem to be more sensitive to them, as manifested by the more frequent intergrowths. We believe that theoretically there is no limit to the n value of these $Sr_{n+1}Ti_nO_{3n+1}$ phases that can be synthesized with MBE. In reality, we are limited by the composition control limits of the AA system and RHEED technique. An attempt to synthesize the $n = 10$ phase resulted in an x-ray diffraction pattern with some diminished and broadened peaks, indicating significant intergrowths.[21]

The growth of epitaxial films allowed the ε_{33} dielectric constant tensor coefficient to be measured in these anisotropic materials. Previous measurements of polycrystalline Sr_2TiO_4 and $Sr_3Ti_2O_7$ samples reported the average dielectric constant (ε_r) to be 38 and 50, respectively.[11] Room temperature dielectric measurements were made on the $n = 1$, 2, and ∞ members of this series with a scanning evanescent microwave microscope (SEMM)[27,28] at 1 GHz and in a parallel plate capacitor structure with an HP 4284A at 1 kHz. The films measured with the SEMM were 1000 Å thick and grown directly on a $(001)LaAlO_3 - Sr_2AlTaO_6$ (LSAT) substrate. LSAT (cubic, $a = 7.737$ Å)[29] has an excellent lattice match with these phases and was used instead of $SrTiO_3$ because its low dielectric constant ($\varepsilon_r = 22.5$)[30] did not interfere with the measurement. The capacitor structures consist of an MBE-grown 1000 Å $Sr_{0.85}La_{0.15}TiO_3$ bottom electrode, a 1000 Å $Sr_{n+1}Ti_nO_{3n+1}$ film, and 0.3 mm diameter Cr/Au top electrodes.

Both of these techniques show excellent agreement for the values of ε_{33}. The first member of this series, Sr_2TiO_4, has a dielectric constant tensor coefficient ε_{33} of 44 ± 4, while $Sr_3Ti_2O_7$ has an ε_{33} of 86 ± 6. The dielectric loss ($\tan\delta$) of all films measured was lower than the detection limit of the SEMM (i.e., less than 1.5%). The magnitude of ε_{33} makes these low n $Sr_{n+1}Ti_nO_{3n+1}$ phases not only of interest for tunable dielectric devices, but also for alternative gate oxides in MOSFETs. Sr_2TiO_4 has several potential ad-

vantages over $SrTiO_3$ in this application including its 38% better lattice match with Si, higher band gap[17] (to reduce leakage), lower thermodynamic driving force for reaction with Si, and greater stability against reduction.

[1] A. Brazdeikis, A. Vailionis, and A. S. Flodstrom, Physica C **235−240**, 711 (1994).

[2] D. G. Schlom, J. N. Eckstein, I. Bozovic, Z. J. Chen, A. F. Marshall, K. E. von Dessonneck, and J. S. Harris, Jr., Proc. SPIE **1285**, 234 (1990).

[3] M. E. Klausmeier-Brown, G. F. Virshup, I. Bozovic, and J. N. Eckstein, Appl. Phys. Lett. **60**, 2806 (1992).

[4] R. Ramesh, S. Jin, and P. Marsh, Nature (London) **346**, 420 (1990).

[5] A. Schilling, M. Cantoni, J. D. Guo, and H. R. Ott, Nature (London) **363**, 56 (1993).

[6] R. J. D. Tilley, J. Solid State Chem. **21**, 293 (1977).

[7] S. N. Ruddlesden and P. Popper, Acta Crystallogr. **10**, 538 (1957); **11**, 54 (1958).

[8] F. W. Van Keuls, R. R. Romanofsky, D. Y. Bohman, M. D. Winters, and F. A. Miranda, Appl. Phys. Lett. **71**, 3075 (1997).

[9] X. X. Xi, H.-C. Li, W. Si, A. A. Sirenko, I. A. Akimov, J. R. Fox, A. M. Clark, and J. Hao, J. Electroceram. **4**, 393 (2000).

[10] R. A. McKee, F. J. Walker, and M. F. Chisholm, Phys. Rev. Lett. **81**, 3014 (1998).

[11] W. Kwestroo and H. A. M. Paping, J. Am. Ceram. Soc. **42**, 292 (1959).

[12] T. Nakamura, P.-H. Sun, Y. J. Shan, Y. Inaguma, M. Itoh, I.-S. Kim, J.-H. Sohn, M. Ikeda, T. Kitamura, and H. Konagaya, Ferroelectrics **196**, 205 (1997).

[13] *Phase Diagrams for Ceramists 1969 Supplement*, edited by E. M. Levin, C. R. Robbins, and H. F. McMurdie (American Ceramic Society, Columbus, 1969), p. 93.

[14] G. J. McCarthy, W. B. White, and R. Roy, J. Am. Ceram. Soc. **52**, 463 (1969).

[15] K. R. Udayakumar and A. N. Cormack, J. Am. Ceram. Soc. **71**, C-469 (1988).

[16] M. A. McCoy, R. W. Grimes, and W. E. Lee, Philos. Mag. A **75**, 833 (1997).

[17] C. Noguera, Philos. Mag. Lett. **80**, 173 (2000).

[18] M. Kawasaki, K. Takahashi, T. Maeda, R. Tsuchiya, M. Shinohara, O. Ishiyama, T. Yonezawa, M. Yoshimoto, and H. Koinuma, Science **266**, 1540 (1994).

[19] J. H. Haeni, C. D. Theis, and D. G. Schlom, J. Electroceram. **4**, 385 (2000).

[20] R. Seshadri, M. Hervieu, C. Martin, A. Maignan, B. Domenges, B. Raveau, and A. N. Fitch, Chem. Mater. **9**, 1778 (1997).

[21] S. Hendricks and E. Teller, J. Chem. Phys. **10**, 147 (1942).

[22] J. B. Nelson and D. P. Riley, Proc. Phys. Soc. London **57**, 160 (1945).

[23] W. Tian, X. Q. Pan, J. H. Haeni, and D. G. Schlom, J. Mater. Res. (to be published).

[24] K. Hawkins and T. J. White, Philos. Trans. R. Soc. London, Ser. A **336**, 541 (1991).

[25] T. Williams, F. Lichtenberg, A. Reller, and G. Bednorz, Mater. Res. Bull. **26**, 763 (1991).

[26] J. Sloan, P. D. Battle, M. A. Green, M. J. Rosseinskz, and J. F. Vente, J. Solid State Chem. **138**, 135 (1998).

[27] C. Gao and X.-D. Xiang, Rev. Sci. Instrum. **69**, 3846 (1998).

[28] H. Chang, I. Takeuchi, and X.-D. Xiang, Appl. Phys. Lett. **74**, 1165 (1999).

[29] D. Mateika, H. Kohler, H. Laudan, and E. Volkel, J. Cryst. Growth **109**, 447 (1991).

[30] S. C. Tidrow, A. Tauber, W. D. Wilber, R. T. Lareau, C. D. Brandle, G. W. Berkstresser, A. J. Ven Graitis, D. M. Potrepka, J. I. Budnick, and J. Z. Wu, IEEE Trans. Appl. Supercond. **17**, 1766 (1997).